OOK/BPSK-Modulated Impulse Transmitters Integrated With Leakage-Cancelling Circuit

Yu-Tsung Lo, Chau-Chan Yui, and Jean-Fu Kiang

***Abstract*—A time-gating technique is adopted to design an on–off keying (OOK) and a binary phase-shift keying (BPSK) ultra-wideband impulse transmitters, respectively. A leakage-cancelling technique is proposed to suppress leakage signal from the oscillator, which is implemented by integrating a leakage-cancelling circuit with the output buffer of the OOK transmitter and the modulator of the BPSK transmitter, respectively. These two types of transmitters have been implemented using 0.18-μm RF CMOS technology. The measured leakage overshoot is less then 1.5 dBc in the OOK transmitter, and is negligible in the BPSK version.**

***Index Terms*—Binary phase-shift keying (BPSK), impulse radio, leakage cancelling, on–off keying (OOK), time gating, transmitter, ultra-wideband (UWB).**

I. Introduction

An IMPULSE radio possesses several advantages over conventional narrowband radios in terms of interference rejection, multipath resolution, and power consumption [1]. In addition, a wideband signal is more difficult to eavesdrop [2]. These properties make ultra-wideband impulse radio (IR-UWB) attractive in radars [3], localization [4], [5], and medical electronics applications [6].

The first ultra-wideband (UWB) impulse signals can be dated back to 1887 when sparks were generated and radiated via wideband dipoles by Hertz [1]. In [7], an impulse is generated using a Hertzian electric dipole. Modern solid-state devices have also been used to generate impulse voltage waveforms to feed the antenna [8].

Current IR-UWB transmitters can be divided into four categories: fast frequency chirp, pulse shaping, up-converting, and time gating. The fast frequency chirp is a frequency-domain method, in which an impulse is generated by sweeping the frequencies of an oscillator [2]. The chirp-based UWB is suitable for impulse radars [2] and middle-low rate wireless communications [9].

In a typical pulse-shaping method, a pulse-shaping filter is connected to the output of a baseband pulse generator (BBPG) to create a more complex pulse waveform. A BBPG, also called a pulse modulator [10], delayed edge combiner [11], or triangular pulse generator [12], is often adopted to generate baseband pulses. It combines two paths of clock signals with different delays, followed by a pulse generation logic. In [13], a third-order Chebyshev filter has been designed in a 0.13-μm CMOS technology to generate a signal with -43 dBm of maximum output power, which meets the Federal Communications Commission (FCC) emission mask of -41.3 dBm. A third-order Bessel filter has also been adopted to meet the same mask [11]. With this method, the passive filter consumes no dc power, but the chip is large and is hardly reconfigurable.

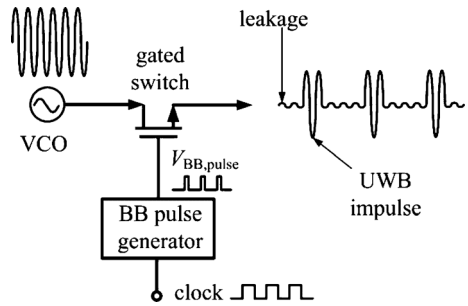

Fig. 1. LO leakage in an impulse transmitter based on time-gating technique.

The up-converting method shapes the baseband pulse by up-converting the local oscillator (LO) carrier to a higher frequency band [14]. The RF transmitter is similar to that in narrowband radios, it requires a voltage-controlled oscillator (VCO) for carrier generation and a mixer for up-conversion.

An IR-UWB radio implemented with the time-gating technique typically consists of an oscillator and a switch. Periodical square-wave pulses are used to control the switch to pass or block the oscillator output signal. The pulse generator can work with different VCOs at different frequencies. However, this technique suffers from LO leakage due to the nonideal off-state of the switches [15].

In this paper, an LO leakage-cancelling technique is proposed to suppress the leakage signals over nonideal switches. Two transmitter chips with on–off keying (OOK) and binary phase-shift keying (BPSK) modulation, respectively, are implemented with the proposed LO cancelling circuit. The leakage-cancelling technique is presented in Section II, circuit designs for the two transmitters are described in Section III, and the measurement results are discussed in Section IV, followed by a conclusion in Section V.

II. LO Leakage-Cancelling Technique

Fig. 1 shows a typical impusle transmitter and the associated LO leakage problem. The baseband signal is used to con-

Manuscript received September 24, 2012; accepted October 13, 2012. Date of publication December 05, 2012; date of current version January 17, 2013. This work was supported by the National Science Council, Taiwan, under Contract NSC 97-2221-E-002-142.

The authors are with the Department of Electrical Engineering and the Graduate Institute of Communication Engineering, National Taiwan University, Taipei 106, Taiwan (e-mail: jfkiang@cc.ee.ntu.edu.tw).

Color versions of one or more of the figures in this paper are available online at http://ieeexplore.ieee.org.

Digital Object Identifier 10.1109/TMTT.2012.2226746

0018-9480/$31.00 © 2012 IEEE

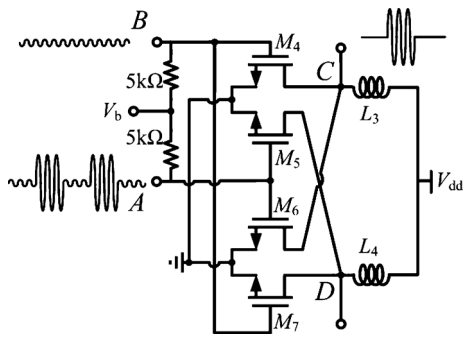

Fig. 2. Illustration of LO leakage-cancelling technique with leakage signals at A and B out of phase.

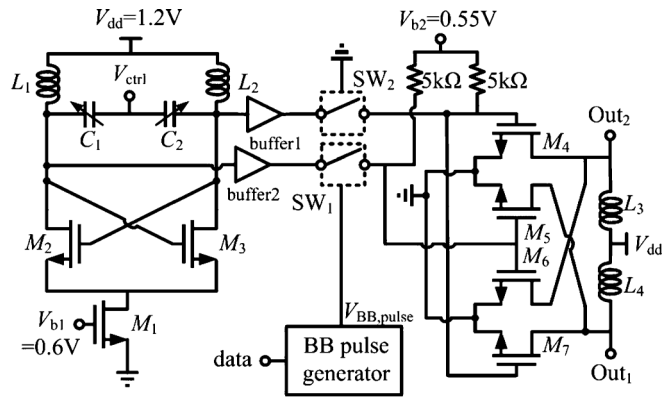

M_1	M_2	M_3	M_4	M_5
60/0.18	15/0.18	15/0.18	33/0.18	33/0.18
M_6	M_7	SW_1	SW_2	L_1
33/0.18	33/0.18	30/0.18	30/0.18	1.3 nH
L_2	L_3	L_4	C_1	C_2
1.3 nH	1.2nH	1.2nH	0.2pF	0.2pF

Fig. 3. Proposed IR-UWB transmitter with OOK modulation.

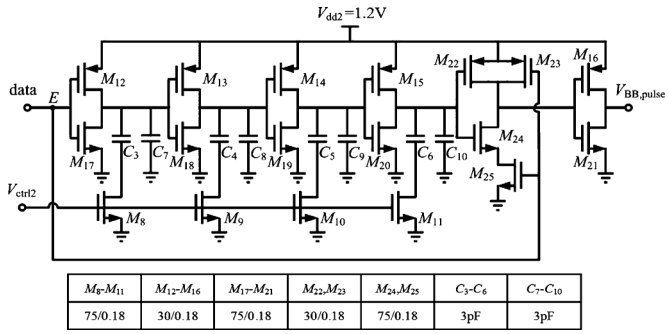

M_8-M_{11}	M_{12}-M_{16}	M_{17}-M_{21}	M_{22},M_{23}	M_{24},M_{25}	C_3-C_6	C_7-C_{10}
75/0.18	30/0.18	75/0.18	30/0.18	75/0.18	3pF	3pF

Fig. 4. BBPG.

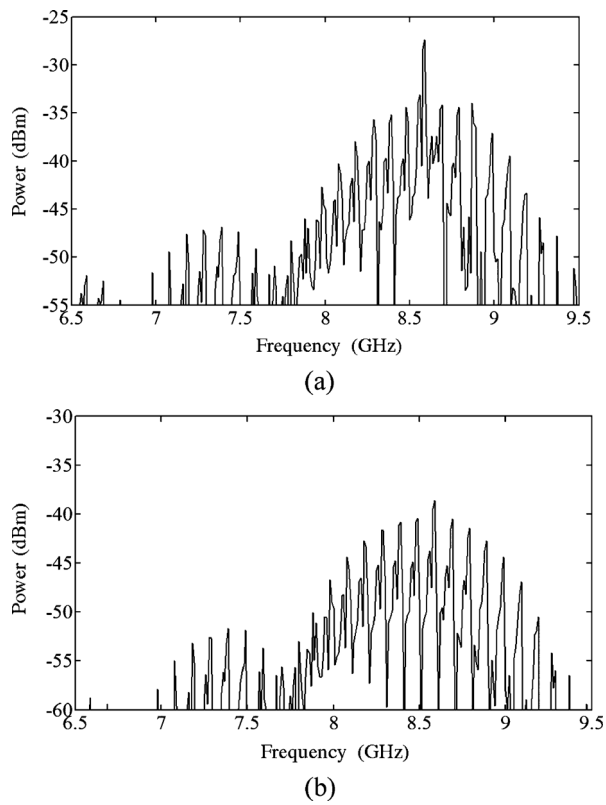

Fig. 5. Simulated spectrum: (a) before and (b) after adding the LO leakage-cancelling circuit.

trol the on/off-state of the switch. The LO leakage due to limited isolation of switches tends to contaminate the spectrum of the intended signal with a strong carrier tone. To design a switch with better isolation usually compromises its insertion loss at the on-state. In [15], two series switches controlled by two pulses with different pulse widths are proposed to reduce the LO leakage. To compensate for the insertion loss due to the additional switches, the output power of the VCO is increased and a buffer is added.

In this work, a leakage-cancelling circuit is designed to generate another signal that is out of phase with the original leakage signal so that the leakage signal can be almost cancelled when the switch is off. When the switch is on, the intended signal is only slightly affected, and the leakage-cancelling capability is not compromised. Another merit is that the leakage-cancelling circuit is integrated with the output buffer; hence, it only takes a little extra dc power.

Fig. 2 shows how the proposed leakage-cancelling technique works. The pulse train goes through the output of the switch to point A when the switch is on, then to the output point C, accompanied by the leakage signal. The output of a dummy switch, which is always at the off-state, is connected to point B.

The differential outputs of the VCO are connected to the baseband-modulated switch and the dummy switch so that the LO leakage signals at points A and B are out of phase. The transistor pairs (M_5, M_6) and (M_4, M_7) transconduct the leakage signals at points A and B, respectively, to currents. By properly routing the drains of these four transistors, the out-of-phase leakage currents add up to zero at the output point C, while their amplitudes are only slightly affected. Note that transistors M_5, M_6, M_4, and M_7 are designed as transconducting elements instead of switches because the leakage signal is usually too small to change the on/off-state of these transistors. The bias voltage is applied to the gate of M_4-M_7 via bias resistors with high resistance.

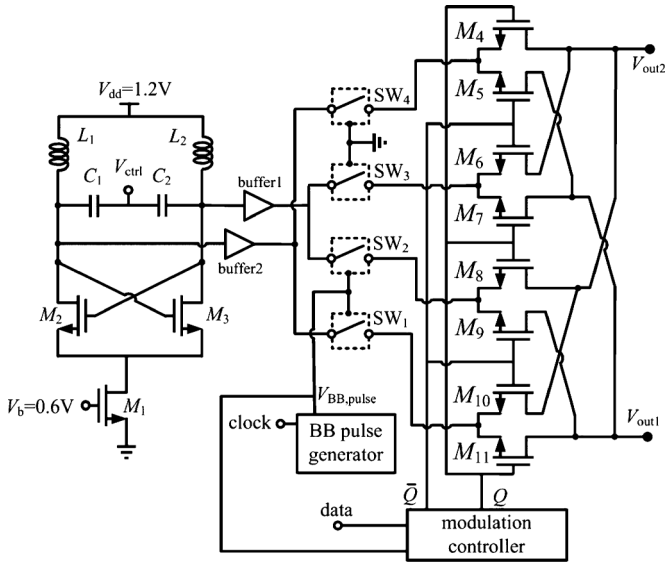

M_1	M_2	M_3	M_4-M_{11}	SW$_1$-SW$_4$
60/0.18	15/0.18	15/0.18	33/0.18	30/0.18
L_1	L_2	C_1	C_2	-
1.3 nH	1.3 nH	0.2pF	0.2pF	-

(a)

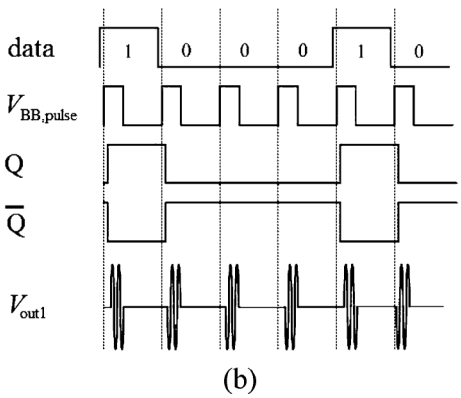

(b)

Fig. 6. Proposed IR-UWB transmitter with BPSK modulation. (a) Schematic. (b) Timing diagram.

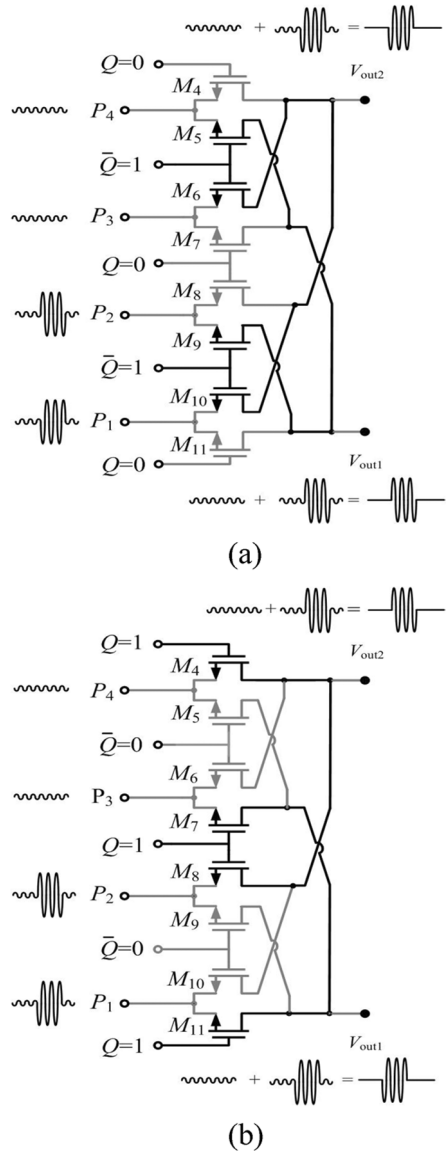

Fig. 7. Illustration of leakage-cancelling process in the BPSK-modulated transmitter. (a) $Q = 0$. (b) $Q = 1$.

III. Circuit Designs

The proposed technique has been applied to an OOK and a BPSK transmitter, respectively, which will be discussed in this section.

A. OOK Transmitter

Fig. 3 shows the OOK-modulated transmitter, which is composed of a BBPG, a VCO with two buffers, two switches, and an output leakage-cancelling circuit, as described in Section II. The sequence of binary data for communication are input to the BBPG, of which the output controls the on/off-state of the baseband-modulated switch SW_1.

The BBPG creates a pulse train with proper duty-cycle. Fig. 4 shows the proposed BBPG, which is composed of an inverter chain and an AND gate. The AND gate is made of a NAND gate and an inverter.

The baseband signal is divided at point E to flow through two separate paths. The signal through one path is delayed by the inverter chains, and that through the other path is directly connected to one input of the NAND gate. The output of the AND gate goes high only when the two input signals are at the high level. The duty cycle of the output signal can be adjusted by proper tuning of the delay. If the pulse repetition rate is 120 MHz and the duty cycle of the BBPG output is 12%, the output pulse width will be about 1 ns.

The delay time of the inverters can be adjusted by loading capacitors. The switches M_8–M_{11} are used to connect the capacitors, C_3–C_6 to ground. A set of fixed capacitors, C_7–C_{10}, are used to provide a fixed delay. The output of the BBPG modulates the switch SW_1, as shown in Fig. 3. Hence, the baseband data is carried as an OOK signal at the output of SW_1.

By connecting the proposed leakage-cancelling circuit as the output buffer of the impule transmitter, the LO leakage at the output of SW_1 is cancelled out. Fig. 5(a) shows the spectrum before adding the LO leakage-cancelling circuit, in which case

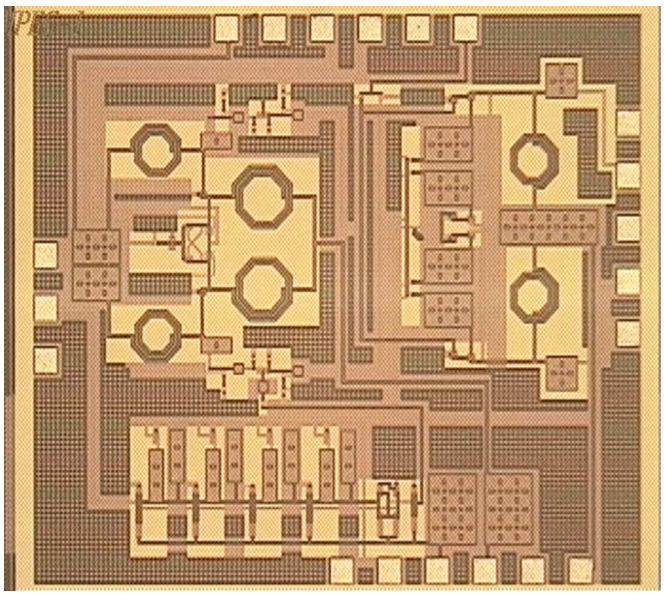

Fig. 8. Chip photograph of OOK-modulated transmitter.

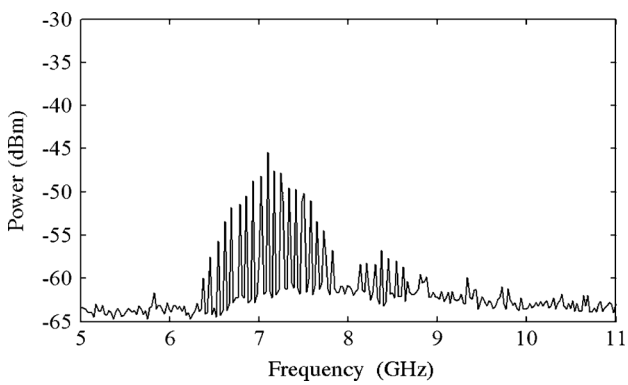

Fig. 9. Measured output spectrum of OOK-modulated transmitter with the VCO tuned to the lowest frequency, $f_{\rm osc} = 7.09$ GHz.

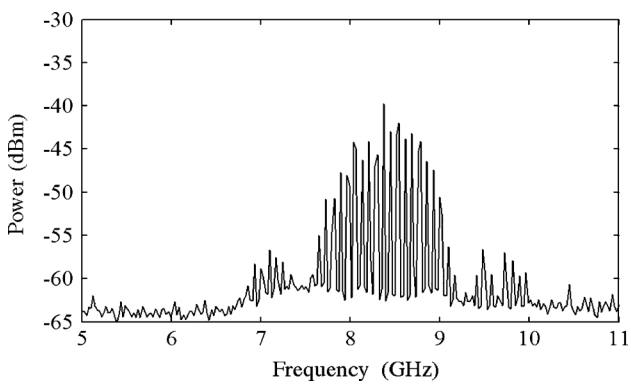

Fig. 10. Measured output spectrum of the OOK-modulated transmitter with the VCO tuned to the highest frequency, $f_{\rm osc} = 8.37$ GHz.

the LO leakage overshoot is around 6 dBc. The leakage-cancelling circuit effectively reduces the overshoot to about 1 dBc, as shown in the Fig. 5(b).

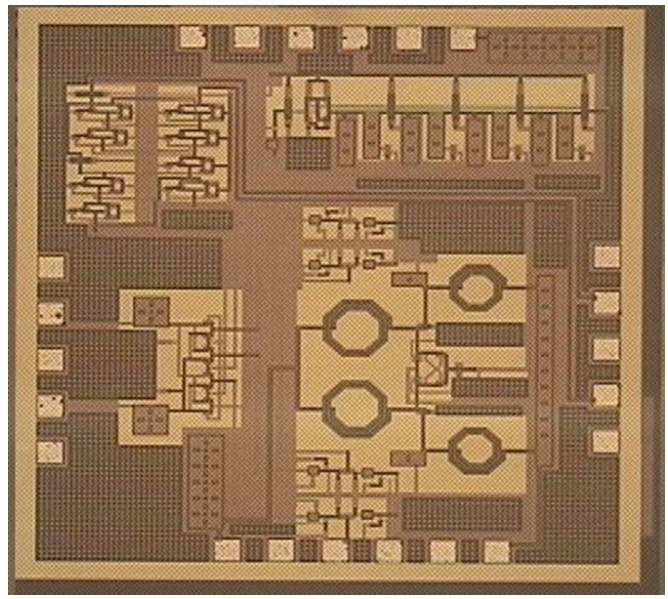

Fig. 11. Chip photograph of BPSK-modulated transmitter.

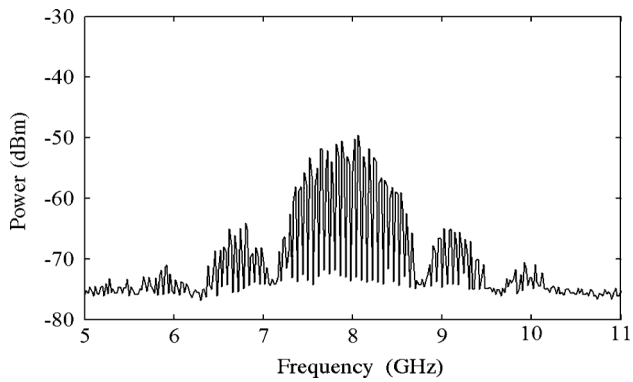

Fig. 12. Measured output spectrum of BPSK-modulated transmitter with the VCO tuned to the highest frequency, $f_{\rm osc} = 8.06$ GHz.

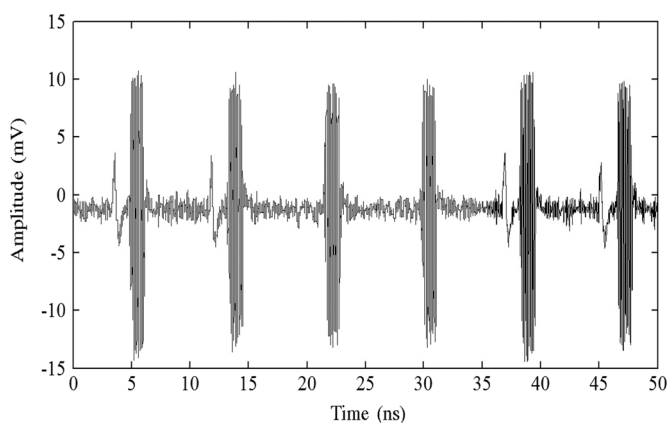

Fig. 13. Measured time-domain signal of BPSK-modulated transmitter.

B. BPSK Transmitter

Fig. 6(a) shows the schematic of the BPSK-modulated transmitter, which is composed of a VCO, four switches, a BBPG, a BPSK modulator with leakage-cancelling circuitry, and a modulation controller made of *D*-flip flops (DFFs).

TABLE I
PERFORMANCE COMPARISON OF UWB IMPULSE TRANSMITTERS

Parameters	BW (GHz)	peak output power (dBm)	PRR (Mpps)[1]	power consump. (mW)	energy cost rate (pJ/pulse)	A (V)	modulation	chip size (mm^2)	process (CMOS)	band (GHz)	technique
This work 1	1.3	−41.5	120	11.8[2]/1.1[3]	98.3[2]/9.2[3]	0.025	OOK	1.37	0.18 μm	6-10	time gating
This work 2	1.1	−50	120	15[2]/1.1[3]	1253[2]/9.2[3]	0.013	BPSK	1.25	0.18 μm	6-10	time gating
CAS-I08 [16]	0.52	−41.3	100	1.68[4]	16.8	0.08	OOK	0.66	0.18 μm	3-5	switching osc.
MTT10 [17]	6.8	−50	100	3.84	38.4	0.71	OOK	0.54	0.18 μm	3-10	pulse shaping
MTT06 [18]	1.2	−39.5	10	1.8	180	0.45	PPM	1.21	0.18 μm	3-5	switching osc.
CAS-II09 [19]	2	−42.7	2	0.236	118	2.45	OOK	0.188[5]	0.18 μm	3-5	switching osc.
JSSC11 [20]	0.5-1.4	−52	50	-	12	0.045	PPM+DB-BPSK	0.032[5]	65 nm	3-5	digital
MTT06 [15]	0.5	−21	15	1.8[6]	120[6]	1	OOK	0.595[5]	0.18 μm	3-10[6]	time gating

[1]: mega-pulses per second, [2]: including power consumption of VCO, [3]: excluding power consumption of VCO, [4]: excluding power consumption of output buffer, [5]: core area, [6]: excluding off-chip signal generator.

The clock signal triggers the BBPG to form a pulse train with proper duty cycle, which is then used to control the switches SW_1 and SW_2.

The VCO and the BBPG are the same as those used in the OOK-modulated transmitter. The switches SW_1 and SW_2 route the two differential outputs, respectively, of the VCO to the BPSK modulator. Switches SW_3 and SW_4 are always at the off-state. The input to SW_1 and SW_4 comes from buffer 2 of the VCO; and the input to SW_2 and SW_3 comes from buffer 1 of the VCO. Note that the output signals of buffers 1 and 2 are 180° out of phase with each other. The output signals from SW_3 and SW_4 are used to cancel the leakage signals at the outputs of SW_1 and SW_2, respectively.

The BPSK modulation controller is designed to select between the two outputs from SW_1 and SW_2. Transistors M_8, M_9, M_{10}, and M_{11} form the core of the BPSK modulator. Transistors M_9 and M_{10} are connected to the inverse output, $\overline{Q}$, of the controller, while M_8 and M_{11} are connected to the positive output, Q.

The clock signal triggers the controller to read the input data. The input data takes the binary return-to-zero (RZ) format, to switch one pair (M_9, M_{10}) on and the other pair (M_8, M_{11}) off, or vice versa. Two BPSK-modulated impulse trains, V_{out1} and V_{out2}, appear at the two output ports, and are out of phase with each other.

Fig. 6(b) shows the timing diagram of the BPSK-modulated transmitter. The data and the baseband pulses are input to the modulation controller made of D-flip-flops; and the output signals Q and $\overline{Q}$ are used to control the BPSK modulator. The core of the BPSK modulator consists of transistors M_8–M_{11}. When $Q = 1, M_8$, and M_{11} are turned on by Q, while M_9 and M_{10} are turned off by $\overline{Q}$. When $Q = 0, M_8$ and M_{11} are turned off, while M_9 and M_{10} are turned on. Hence, the phase of the output signal V_{out1} is 0° when the baseband data is 1, and is 180° when the baseband data is 0. The beseband data are thus transformed to BPSK signals for transmission.

The proposed leakage-cancelling technique applied to the OOK transmitter can be modified to adopt in the BPSK transmitter. Fig. 7(a) and (b) shows the BPSK modulation scheme with $Q = 0$ and $Q = 1$, respectively. Transistors M_4–M_7 are used to cancel the LO leakage in the core of the BPSK modulator made of transistors M_8–M_{11}. Switches SW_3 and SW_4 are always at the off-state, passing only leakage signals to M_4–M_7.

First, consider V_{out1} as the output port. At $Q = 1, M_7$ and M_{11} are on, the leakage from P_1 is cancelled by the leakage from P_3. At $Q = 0, M_5$ and M_9 are on, the leakage from P_2 is cancelled by the leakage from P_4. Similarly, consider V_{out2} as the output port: At $Q = 1, M_4$ and M_8 are on, the leakage from P_2 is cancelled by the leakage from P_4. At $Q = 0, M_6$ and M_{10} are on, the leakage from P_1 is cancelled by the leakage from P_3. Either V_{out1} or V_{out2} can be used for BPSK impulse transmission, and a differential mode can be operated if both are used.

In the OOK transmitter, the leakage-cancelling circuit provides transconductance. Inductors L_3 and L_4 in Fig. 3 are used to tune the output matching around 8 GHz. In the BPSK transmitter, transistors M_4–M_7 make up the leakage-cancelling circuit, and M_8–M_{11} make up the modulator core with all eight transistors controlled by signals Q and $\overline{Q}$. Since M_4–M_{11} function like switches, no additional dc power consumption is incurred.

IV. MEASUREMENTS AND DISCUSSIONS

Fig. 8 shows a chip photograph of the OOK-modulated transmitter, which is fabricated using TSMC 0.18-μm CMOS

technology. The chip size is 1.27×1.08 mm^2. When operated at the PRR of 120 Mb/s, the power consumption is 11.8 mW, among which the VCO consumes 10.68 mW, and $V_{dd} = 1.2$ V.

Figs. 9 and 10 show the measured output spectra at the lowest and the highest VCO frequencies, respectively. The output 10-dB bandwidths are 1.3 and 1.25 GHz, respectively. The VCO frequency $f_{\rm osc}$ can be tuned over the range from $f_{\rm osc} = 7.09$ GHz at $V_{\rm ctrl} = 0$ V to 8.37 GHz at $V_{\rm ctrl} = 1.8$ V. It is observed that the LO leakage overshoot has been reduced to about 1.5 dBc above the signal spectrum in both figures. The peak output power in Figs. 9 and 10 are -45.45 and -41.51 dBm, respectively, lower than the FCC ceiling of -41.3 dBm.

Fig. 11 shows a chip photograph of the BPSK-modulated transmitter, which is also fabricated using TSMC 0.18-μm CMOS technology. The chip has the size of 1.16×1.08 mm^2, and consumes 15 mW of dc power with $V_{dd} = 1.2$ V.

Fig. 12 shows the measured output spectrum at $f_{\rm osc} = 8.06$ GHz. The 10-dB bandwidth is 1.1 GHz. The LO leakage has been suppressed to a level barely observable.

Fig. 13 shows the measured time-domain signal with BPSK modulation. The pulse train follows the timing diagram, as shown in Fig. 6(b). The spikes are due to the phase transition of the BPSK signal.

Table I summarizes the performance of the two transmitters and their comparison with literatures. All the works, except [15], have their peak output power lower than -41.3 dBm [14]. To meet this FCC regulation, an UWB transmitter can generate pulses of large amplitude and low duty cycle, or pulses of small amplitude and high duty cycle. The former one can cover a larger area at the cost of lower throughput [21]. For example, both [19] and this OOK-modulated transmitter have peak output power of -42 dBm. The large amplitude of 2.45 V in [19] restrains its maximum allowable PRR to 2 Mp/s, while the low amplitude of 25 mV in the proposed OOK-modulated transmitter allows its PRR up to 120 Mp/s.

V. Conclusion

Two types of IR-UWB transmitters have been designed on a time-gating technique. To reduce the leakage from the LO, leakage-cancelling circuits have been embedded to the output buffer of the OOK transmitter, and integrated with the modulator of the BPSK transmitter. This technique can be applied to time-gating impulse transmitters, without resorting to a tradeoff between the leakage-cancelling capability and the insertion loss. The simulated and measured performance confirms the effectiveness of this cancelling technique.

Acknowledgment

The authors would like to acknowledge fabrication support provided by National Chip Implementation Center (CIC), Hsinchu, Taiwan.

References

[1] M. Z. Win, D. Dardari, A. F. Molisch, W. Wiesbeck, and J. Zhang, "History and applications of UWB," *Proc. IEEE*, vol. 97, no. 2, pp. 198–204, Feb. 2009.

[2] I. Oppermann, M. Hämäläinen, and J. Iinatti, *UWB: Theory and Applications*. New York: Wiley, 2004.

[3] Y. Kawano, Y. Nakasha, K. Yokoo, S. Masuda, T. Takahashi, T. Hirose, Y. Oishi, and K. Hamaguchi, "RF chipset for impulse UWB radar using 0.13 μm InP-HEMT technology," *IEEE Trans. Microw. Theory Techn.*, vol. 54, no. 12, pp. 4489–4497, Dec. 2006.

[4] D. Martynenko, G. Fischer, and O. Klymenko, "A high band impulse radio UWB transmitter for communication and localization," in *IEEE Int. Ultra-Wideband Conf.*, Vancouver, BC, Canada, Sep. 2009, pp. 359–363.

[5] Y. J. Zheng *et al.*, "A 0.92/5.3 nJ/b UWB impulse radio SoC for communication and localization," in *IEEE Int. Solid-State Conf.*, Feb. 2010, pp. 230–231.

[6] T. Nakagawa, G. Ono, R. Fujiwara, T. Norimatsu, T. Terada, and M. Miyazaki, "Fully integrated UWB-IR CMOS transceiver for wireless body area networks," in *IEEE Int. Ultra-Wideband Conf.*, Vancouver, BC, Canada, Sep. 2009, pp. 768–772.

[7] M. G. M. Hussain, "Antenna patterns of nonsinusoidal waves with the time variation of a Gaussian pulse," *IEEE Trans. Electronmagn. Compat.*, vol. 31, no. 1, pp. 48–54, Feb. 1989.

[8] V. V. Kulkarni, M. Muqsith, K. Niitsu, H. Ishikuro, and T. Kuroda, "A 750 Mb/s, 12 pJ/b, 6-to-10 GHz CMOS IR-UWB transmitter with embedded on-chip antenna," *IEEE J. Solid-State Circuits*, vol. 44, no. 2, pp. 394–403, Feb. 1997.

[9] J. Zhang, H. Y. Hu, R. Z. Kang, and X. Li, "Transmitted-reference chirp ultra-wideband (UWB) wireless communication system," in *Int. Future Computer Commun. Conf.*, Wuhan, China, May 2010, vol. 2, pp. V2-674–680.

[10] Y. Nakasha *et al.*, "W-band transmitter and receiver for 10-Gb/s impulse radio with an optical-fiber interface," *IEEE Trans. Microw. Theory Techn.*, vol. 57, no. 12, pp. 3171–3180, Dec. 2009.

[11] S. Bourdel *et al.*, "A 9-pJ/pulse 1.42-Vpp OOK CMOS UWB pulse generator for the 3.1–10.6-GHz FCC band," *IEEE Trans. Microw. Theory Techn.*, vol. 58, no. 1, pp. 65–72, Jan. 2010.

[12] S. Bagga *et al.*, "Codesign of an impulse generator and miniaturized antennas for IR-UWB," *IEEE Trans. Microw. Theory Techn.*, vol. 54, no. 4, pp. 656–1666, Jun. 2006.

[13] Y. Bachelet *et al.*, "Fully integrated CMOS UWB pulse generator," *IET Electron. Lett.*, vol. 42, no. 22, pp. 1277–1278, Oct. 2006.

[14] D. D. Wentzloff and A. P. Chandrakasan, "Gaussian pulse generators for subbanded ultra-wideband transmitters," *IEEE Trans. Microw. Theory Techn.*, vol. 54, no. 4, pp. 1647–1655, Jun. 2006.

[15] R. Xu, Y. Jin, and C. Nguyen, "Power-efficient switching-based CMOS UWB transmitters for UWB communications and radar systems," *IEEE Trans. Microw. Theory Techn.*, vol. 54, no. 8, pp. 3271–3277, Aug. 2006.

[16] A. T. Phan, J. Lee, V. Krizhanovskii, Q. Le, S. K. Han, and S. G. Lee, "Energy-efficient low-complexity CMOS pulse generator for multiband UWB impulse radio," *IEEE Trans. Circuits Syst. I, Reg. Papers*, vol. 55, no. 11, pp. 3552–3563, Dec. 2008.

[17] S. Bourdel, Y. Bachelet, and J. Gaubert, "A 9-pJ/Pulse 1.42-Vpp OOK CMOS UWB pulse generator for the 3.1 V10.6-GHz FCC band," *IEEE Trans. Microw. Theory Techn.*, vol. 58, no. 1, pp. 65–73, Jan. 2010.

[18] D. Barras, F. Ellinger, H. Jackel, and W. Hirt, "Low-power ultra-wideband wavelets generator with fast start-up circuit," *IEEE Trans. Microw. Theory Techn.*, vol. 54, no. 5, pp. 2138–2145, May 2006.

[19] S. Diao, Y. Zheng, and C. H. Heng, "A CMOS ultra low-power and highly efficient UWB-IR transmitter for WPAN applications," *IEEE Trans. Circuits Syst. II, Exp. Briefs*, vol. 56, no. 3, pp. 200–204, Mar. 2009.

[20] Y. Park and D. D. Wentzloff, "An all-digital 12 pJ/pulse IR-UWB transmitter synthesized from a standard cell library," *IEEE J. Solid-State Circuits*, vol. 46, no. 5, pp. 1147–1157, May 2011.

[21] J. Foerster, E. Green, S. Somayazulu, and D. Leeper, "Ultra-wideband technology for short- or medium-range wireless communications," *Intel Tech. J.*, vol. Q2, pp. 1–11, 2001.

Yu-Tsung Lo was born in Taipei, Taiwan, on March 11, 1985. He received the B.S. degree in electrical engineering and M.S. degree in communication engineering from National Taiwan University, Taipei, Taiwan, in 2007 and 2009, respectively, and is currently working toward the Ph.D. degree at NTU.

Since 2010, he has been with the National Chip Implementation Center (CIC), Hsinchu, Taiwan, where he is engaged in RF integrated circuit (RFIC) and device measurements. His research interests include CMOS RFICs, microwave systems and measurements, and UWB technology.

Chau-Chan Yui, photograph and biography not available at time of publication.

Jean-Fu Kiang was born in Taipei, Taiwan, on February 2, 1957. He received the B.S. and M.S. degrees from National Taiwan University, Taipei, Taiwan, in 1979 and 1981, respectively, and the Ph.D. degree from the Massachusetts Institute of Technology, Cambridge, in 1989, all in electrical engineering.

In 1985 and 1986, he was with Schlumberger-Doll Research, Ridgefield, CT. From 1989 to 1990, he was with the IBM Watson Research Center, Yorktown Heights, NY. From 1990 to 1992, he was with Bellcore, Red Bank, NJ. From 1992 to 1994, he was with Siemens Electromedical Systems, Danvers, MA. From 1994 to 1999, he was with National Chung-Hsing University, Taichung, Taiwan. Since 1999, he has been a Professor with the Department of Electrical Engineering and the Graduate Institute of Communication Engineering, National Taiwan University. He has been interested in electromagnetic applications and system issues, including wave propagation in the ionosphere and the atmosphere, antennas, satellite navigation, remote sensing, and RF module and transceiver design.